CONTACT INFORMATION
Mining Records Curator
Arizona Geological Survey
416 W. Congress St., Suite 100
Tucson, Arizona 85701
520-770-3500
http://www.azgs.az.gov
inquiries@azgs.az.gov

The following file is part of the

James Doyle Sell Mining Collection

ACCESS STATEMENT

These digitized collections are accessible for purposes of education and research. We have indicated what we know about copyright and rights of privacy, publicity, or trademark. Due to the nature of archival collections, we are not always able to identify this information. We are eager to hear from any rights owners, so that we may obtain accurate information. Upon request, we will remove material from public view while we address a rights issue.

CONSTRAINTS STATEMENT

The Arizona Geological Survey does not claim to control all rights for all materials in its collection. These rights include, but are not limited to: copyright, privacy rights, and cultural protection rights. The User hereby assumes all responsibility for obtaining any rights to use the material in excess of "fair use."

The Survey makes no intellectual property claims to the products created by individual authors in the manuscript collections, except when the author deeded those rights to the Survey or when those authors were employed by the State of Arizona and created intellectual products as a function of their official duties. The Survey does maintain property rights to the physical and digital representations of the works.

QUALITY STATEMENT

The Arizona Geological Survey is not responsible for the accuracy of the records, information, or opinions that may be contained in the files. The Survey collects, catalogs, and archives data on mineral properties regardless of its views of the veracity or accuracy of those data.

Arizona Geological Society Digest, Volume X, March 1976

INTERNAL STRUCTURE AND MECHANISM OF EMPLACEMENT OF A SMALL GRAVITY-GLIDE SHEET, SAGUARO NATIONAL MONUMENT (EAST), TUCSON, ARIZONA [1]

by

George H. Davis

Department of Geosciences,
University of Arizona, Tucson

and

Eric G. Frost

Department of Geological Sciences,
University of Southern California, Los Angeles

Abstract

Deformational features in Paleozoic limestone and shale within Saguaro National Monument (East) near Tucson, Arizona have been interpreted by McColly (1961) and Davis (1973, 1975) as products of gravity gliding. Large-scale (1:120) geologic mapping in a portion of the Monument area disclosed an array of folds and folded faults whose characteristics provide insights regarding the gliding mechanism. The rocks were found to consist of five folded imbricate plates. Within the deformed sequence, there is a downward increase in the frequency and tightness of folds in each plate and in the degree of folding of the fault boundaries of each plate. The folded fault-boundaries coincide with shale-rich layers pervaded by bedding-plane cleavage, overturned folds, isoclinal recumbent rootless folds, boudinage, and slickensides.

Kehle's (1970) multiple-décollement, rheological model of gravity gliding explains to a remarkable degree the mechanical processes responsible for the observed deformation. Gravity gliding took place by incremental movements during which folding and faulting were synchronous. Low-angle tectonic transport of relatively brittle limestone layers was carried out by shear flow of an underlying, low-viscosity, shale-rich zone. Repetition of the section was achieved by buttressing effects superseded by step thrusting during the sustained simple-shear flow of the chief shale-rich décollement zone.

Introduction

The Tanque Verde and Rincon Mountains east of Tucson, Arizona consist predominantly of an assemblage of banded augen gneiss and gneissic granitic rocks that include the Catalina Gneiss of Moore and

---

[1] Contribution No. 699, Department of Geosciences, University of Arizona, Tucson, Arizona.

others (1941) and the Wrong Mountain quartz monzonite and Continental granodiorite of Drewes (1972). Although of Precambrian origin, these rocks became mobile during a Mesozoic-Cenozoic metamorphism and were emplaced as part of a diapiric domal uplift into a Precambrian metasedimentary and Phanerozoic sedimentary cover (Mayo, 1964; Davis and others, 1975). At present, the gneissic complex exposed in the Tanque Verde and Rincon Mountains is stripped of all the Paleozoic and Mesozoic rocks that it had once domed, except locally around the base of the mountains where thin sheets of sedimentary rocks rest subconcordantly and in fault contact on the granitic gneiss. The contact, known as the Catalina fault (Pashley, 1966), is gently dipping and generally conforms to the attitude of foliation in the gneissic rocks. The Catalina fault separates rocks of strikingly dissimilar geologic provenance.

One of us (Davis, 1973; 1975) has presented evidence that the Paleozoic-Mesozoic sedimentary rocks on the hanging wall of the Catalina fault represent remnants of gravity-glide sheets that moved radially away from the culmination of the gneissic complex sometime in the Tertiary. The convex upper surface of the gneissic complex, i.e., the Catalina fault, was interpreted as a décollement above which the sedimentary rocks glided and folded independently of the crystalline substratum.

In an effort to define the mechanical processes responsible for gravity gliding of the sheets of sedimentary and metasedimentary rocks, the deformational characteristics of part of one of the glide sheets located in Saguaro National Monument (East) were examined in some detail. Although small in area (8,000 m^2), the study site is representative of most of the glide sheets in the Rincon Mountain area (Davis, 1975) in that it contains a gently dipping, thin sheet of folded sedimentary rocks resting in fault contact on the gently dipping surface of the gneissic rocks. The rocks examined are located at the base of the exposed western limb of the Tanque Verde antiform, an upright, symmetrical, east-northeast-trending fold in the gneiss. The structural geology within the study site is extraordinarily complex. However, the unraveling of aspects of this complexity through geologic mapping and application of Kehle's (1970) distributed shear model provides insight into the characteristics of one type of gravity-glide system that was operative in the Rincon Mountain area.

Previous Work

Moore and others (1941) first examined the sedimentary rocks within Saguaro National Monument. They assigned these rocks to the Cretaceous System and attributed the deformed state of the rocks to eastward-directed regional overthrusting. McColly (1961) mapped the geology of Saguaro National Monument and concluded that the sedimentary rocks assumed their present position and structural configuration through landsliding off Tanque Verde Mountain. McColly noted the presence of a large S-shaped overturned fold which he interpreted to indicate movement directed westward off the mountain. Davis (1975) studied the folds in Saguaro National Monument and interpreted them as products of N. 50° W.-directed gravity gliding. The extreme deformation by folding suggested to Davis that gliding took place at depth (perhaps 2 to 3 km ?) and was related to the structural high represented by the Tanque Verde antiform. Drewes (1972, 1975) mapped the geology of the Rincon and Tanque Verde Mountains, including Saguaro National Monument. He has postulated that the Paleozoic and Mesozoic sedimentary rocks exposed on the flanks of the Tanque Verde and Rincon Mountains are remnants of regionally extensive allochthons emplaced by thrust faulting during the Laramide (Drewes, 1973). Drewes regards the gravity-induced tectonic features as superimposed on the thrust-faulted strata.

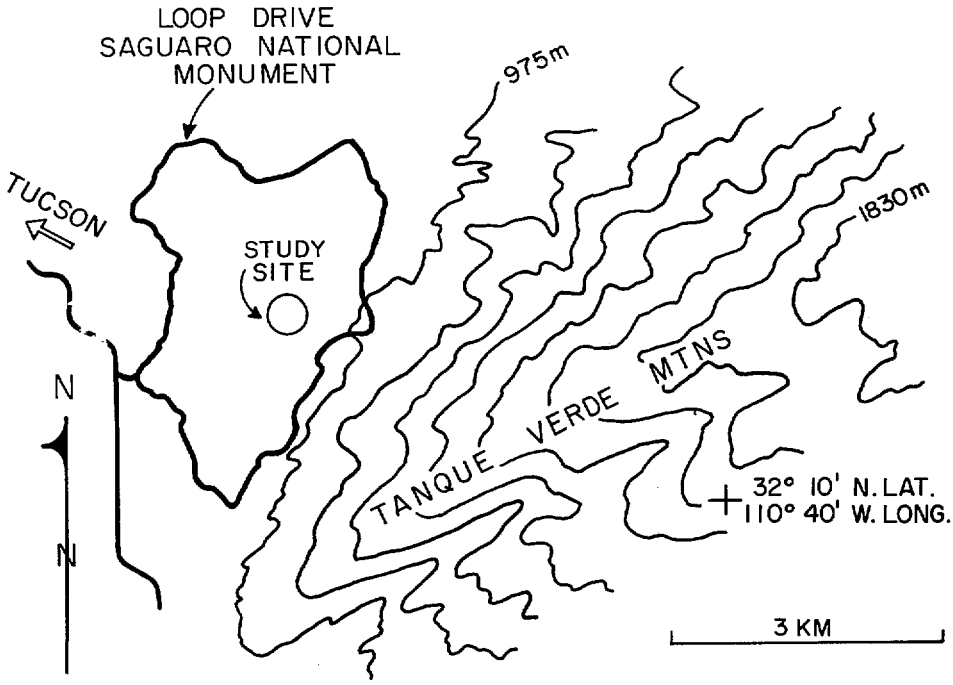

Figure 1. Location of study area.

Location and Methods

The area selected for detailed examination is located within the Loop Drive in Saguaro National Monument (Fig. 1). Reconnaissance mapping of rocks in this study area disclosed that the "S-shaped fold" mapped by McColly (1961) does not exist, although the outcrop pattern suggests the presence of such a structure (Fig. 2). Units could not be traced from the upper limb to the overturned middle limb of the fold, nor could units be traced from the vertical part of the middle limb to the lower limb. In order to define more rigorously the structural configuration of rocks in the study area, geologic mapping was carried out at a scale of 1:120, using plane table and alidade for control (Davis and others, 1974). For mapping purposes, approximately twenty-five lithologic units were distinguished.

Rocks

Sedimentary rocks exposed in the study area were interpreted tentatively by McColly (1961, p. 31-40) as belonging to the Pennsylvanian–Permian Earp Formation. The rocks are highly deformed and generally unfossiliferous, rendering the assignment of formation name and age difficult. The relatively high percentage of shale layers within the section is consistent with the general lithologic properties of the Earp Formation. During the course of our geologic studies within the study area, we have inferred that the sedimentary rocks are late Paleozoic in age and probably do indeed belong to the Earp Formation.

The rocks consist chiefly of shale, limestone, and siltstone which comprise a sedimentary sheet no thicker than 75 m. Several hundred meters east of the study area, the sheet of sedimentary rock rests concordantly on the well-exposed, homoclinally dipping upper surface of Catalina Gneiss,[1] which there is inclined approximately 15° to 20° NW. Within the study area, the sedimentary sheet dips an average of 35° NE and is inferred to be slightly discordant to the attitude of foliation in the underlying gneiss.

Five lithologic units within the sequence of rocks in the study area are portrayed on the geologic map (Plate 4, in pocket), and these are described in Table 1. It has been assumed, but not proved, that this section is right side up. Unit 1 consists of at least 45 m of very fissile shale containing thin layers, tectonic slices, and rootless folds of brown siltstone and orange dolomite. The unit is highly deformed and its base is nowhere exposed. The upper surface of the Catalina Gneiss is inferred to lie at a depth of approximately 20 m below unit 1. Unit 2 is approximately 3 m thick and consists of a very black to dark-gray-weathering micrite bed overlain by mudstone. The micrite is distinctive because of its ribbonlike, thin-bedded appearance. It contains abundant calcite veinlets, as well as several mudstone partings. Unit 3 is approximately 2 m thick and is dominated by thin-bedded, black to dark-gray micrite with mudstone partings and abundant calcite veinlets. At the base of unit 3 is a very fine grained, pink, silty limestone which grades upward into a medium- to light-gray micrite bed containing brown chert stringers. Unit 4 consists of approximately 2 m of resistant interbedded black and gray to brown micrite with abundant calcite veinlets. Thin beds can be discerned on weathered surfaces. The upper portion of the micrite is medium to light gray, irregularly fractured, and smooth weathering. The base of unit 4 is marked by a layer of calcareous mudstone which varies

---

[1] "Catalina Gneiss" is used herein merely as a general term for the crystalline, granitic-gneissic rocks in the Tanque Verde Mountains.

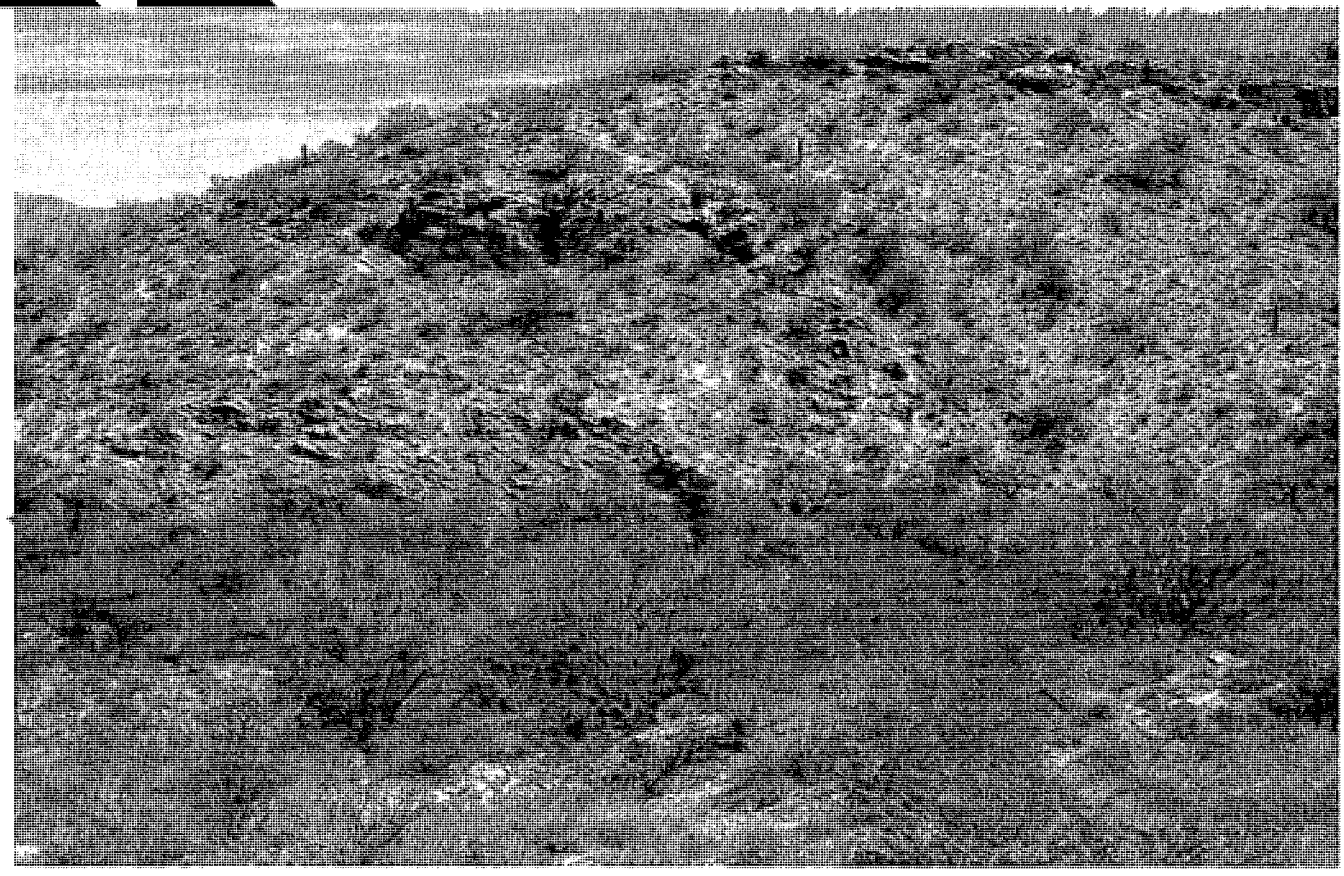

Figure 2. Photograph of portion of study area (view to north) showing apparent "S-shape" configuration of the relatively resistant limestone units.

Table 1. Marker units recognized in the portion of the Pennsylvanian-Permian Earp (?) Formation exposed in the study area.

Unit	Approximate Thickness	Lithologic Description
5	1.2 m	Micrite, medium to light gray, moderately well developed ribbonlike bedding, highly fractured.
	0.5 m	Micrite, medium to light gray, massive, smooth weathering, abundant white calcite veinlets parallel to bedding.
	0.6 m	Micrite, interbedded brown and black; upper portion thin bedded, highly fractured, and containing minor brown chert; lower portion resistant and containing prominent brown layer at base.
	0.6 m	Micrite, medium to light gray, highly fractured, white calcite vein fillings.
	0.6 m	Micrite, black, massive, some surfaces smooth weathering with brown coating and tiny black splotches (?).
	0.5 m	Micrite, medium to light gray, smooth weathering, ribbonlike "flowage" texture.
4	0.3 m	Mudstone, forms pronounced parting.
	0.3 m	Micrite, medium to light gray, irregularly fractured, punky.
	1.2 m	Micrite, interbedded black and gray-brown, thin bedding accentuated on weathered surfaces, abundant calcite stringers.
	0.2 m	Mudstone, buff, brown, green, pink, calcareous, nonresistant.
3	0.3 m	Micrite, gray, thin bedded, contains mudstone partings.
	0.9 m	Micrite, black to dark gray, thinly bedded, ribbonlike on weathered surfaces, thin gray interbeds.
	0.6 m	Micrite, gray-white, thin bedded, some resistant white mudstone layers, abundant calcite veinlets.
	0.2 m	Silty limestone, very fine grained, pink, platy with paper-thin layers, minor chert stringers, gradational between overlying micrite and underlying mudstone.

Table 1. Marker units--Continued

Unit	Approximate Thickness	Lithologic Description
2	1.2 m	Mudstone, light brown to green, uppermost 6 cm are pronounced green, very thin bedded with silty layers, calcareous, nonresistant, gradational contacts.
	0.15 m	Micrite, black, thin bedded, white to green mudstone partings.
	0.45 m	Micrite, black, massive, abundant calcite lenses.
	1.2 m	Micrite, mostly very black, some weathers gray, ribbonlike weathered appearance, wavy or crinkled bedding, thin mudstone partings abundant, calcite stringers.
1	1.0 m	Shale, maroon, pervasive bedding-plane cleavage, rootless folds of siltstone and dolomite.
	0.5 m	Dolomite, white with pink or orange hue, granular, weathers to relatively smooth surfaces with orange-brown chert stringers.
	43(?) m	Shale, maroon and brown, very fissile, tectonic slices of brown siltstone, bedding-plane cleavage, rootless folds.

Total thickness measured = 55.5 m

in color from buff to green to pink. The top of unit 4 is a thin mudstone parting which is distinctive because of the extent to which it weathers back into the hillsides, creating overhanging ledges. Unit 5 is a 4-m thick, resistant micrite bed which varies in color from black to medium to light gray. Weathered surfaces of the micrite beds in unit 5 are typically smooth, but some of the layers display a laminated, ribbonlike appearance.

Internal Structure

Large-scale geologic mapping of individual marker units disclosed the presence of at least four low-angle faults along which portions of the section have been quadrupled. The faults have been folded, as have the sedimentary rocks forming each plate between the faults.

Evidence for low-angle tectonic transport within the map area is conspicuous and consists of (1) overturned folds (Fig. 3), (2) isoclinal rootless folds with axial surfaces parallel to bedding, (3) bedding-plane cleavage (Fig. 4), (4) low-plunging slickensides on bedding surfaces, (5) subhorizontal boudinage and tectonic slices (Fig. 5), (6) displacement of calcite veinlets along small-scale, low-angle, bedding-plane faults, (7) repetition of section, and (8) low-angle faults.

The uppermost plate (plate 5 in Plate 4) consists of units 2 to 5 and is deformed by relatively low-amplitude, long-wavelength folds on the west and high-angle normal faults on the east. The broad folds recognized in plate 5 plunge approximately 40° NE and are characterized by nearly vertical axial surfaces. Several overturned folds within unit 5 were observed, and these are asymmetric northwestward. Axial surfaces of the folds strike north-northwest and dip moderately east-northeast. Axes of the folds plunge approximately 30° NNE. Vertical calcite veins in unit 5 are offset by bedding-plane slip surfaces; successively higher beds are displaced westward. The normal faults in the eastern part of plate 5 generally strike north-northeast and dip east-southeast at angles ranging from 20° to 65°. Slickensides are dip slip. On the east, the low-angle fault at the base of plate 5 coincides with the contact between units 1 and 2. Westward the fault steps up section and follows the mudstone bed at the base of unit 4. Farther west the fault steps up into unit 5. Both the fault and the enveloping surface of folds contained in plate 5 appear to be smoothly arched about gently north-northeast-plunging axes.

Plate 4 is composed predominantly of units 4 and 5, but two anticlinal folds in the western part of this plate contain exposures of units 1 to 3 (Plate 4). Deformation by folding is well developed in plate 4. The folds are tighter and more numerous than those in plate 5. They vary from markedly overturned to upright, with axial surfaces striking north-northwest and dipping from 30° to 80° ENE. Axes of the folds plunge gently to moderately north-northeast. Axial traces of the folds are spaced every 3 to 6 m. Individual overturned folds that can be traced northwesterly become upright (Plate 4). The low-angle fault at the base of plate 4 is strongly curviplanar. Along the southwest margin of the plate, the fault strikes northwest, dips approximately 30° NE, and separates plates 3 and 4. Along the eastern margin of plate 4, the fault dips approximately 70° W and truncates rocks of plate 2. Thus, the low-angle fault at the base of plate 4 (and the plate itself) seems to be folded into a syncline whose axis plunges gently to the north. At the northeastern corner of plate 4 (Plate 4), the low-angle fault at the base of the plate is truncated by the fault at the base of plate 5.

Plate 3 contains units 3 to 5 and is characterized by tight overturned and recumbent folds. Overturning is northwesterly (Plate 4).

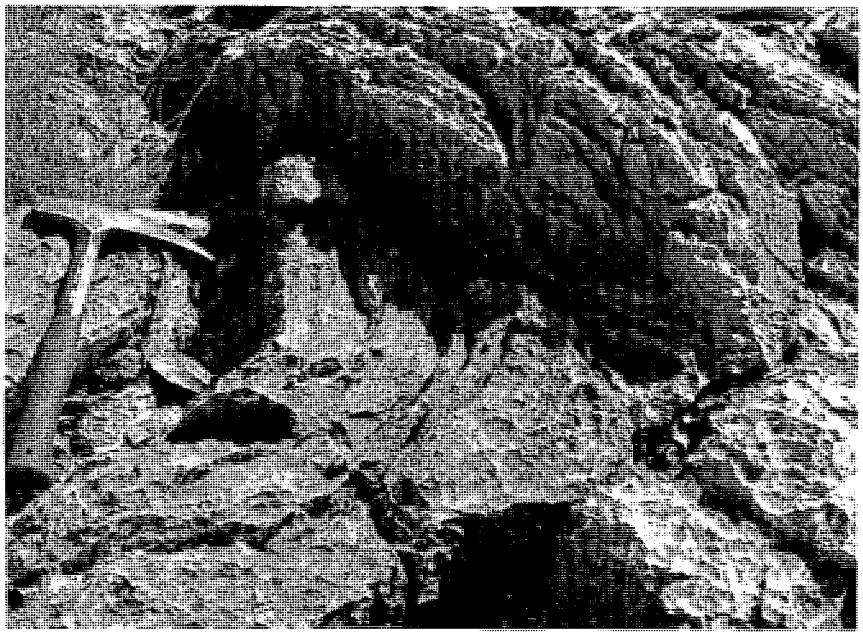

Figure 3. Overturned syncline in limestone, unit 5, plate 3, looking north.

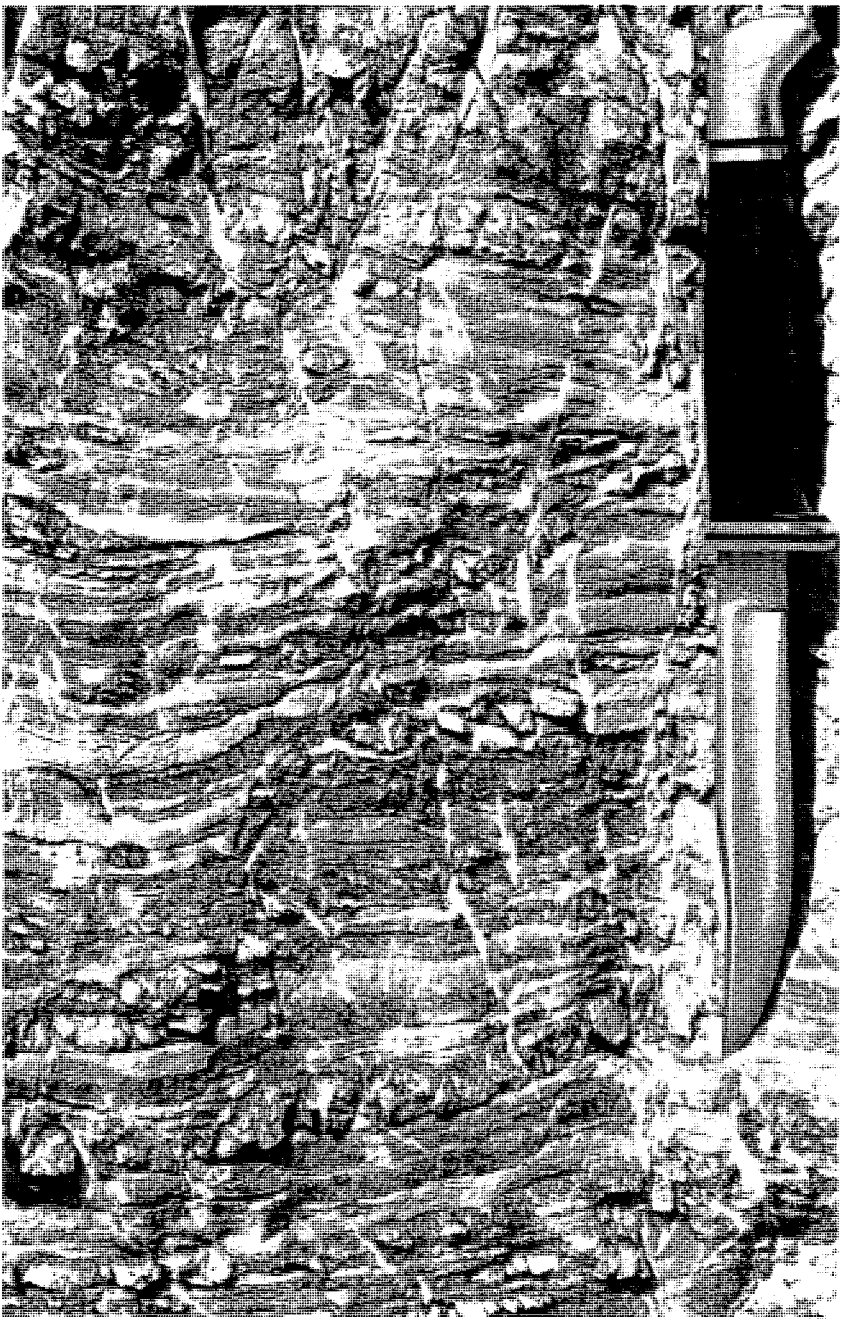

Figure 4. Bedding-plane cleavage in thinly laminated dolomite of unit 1.

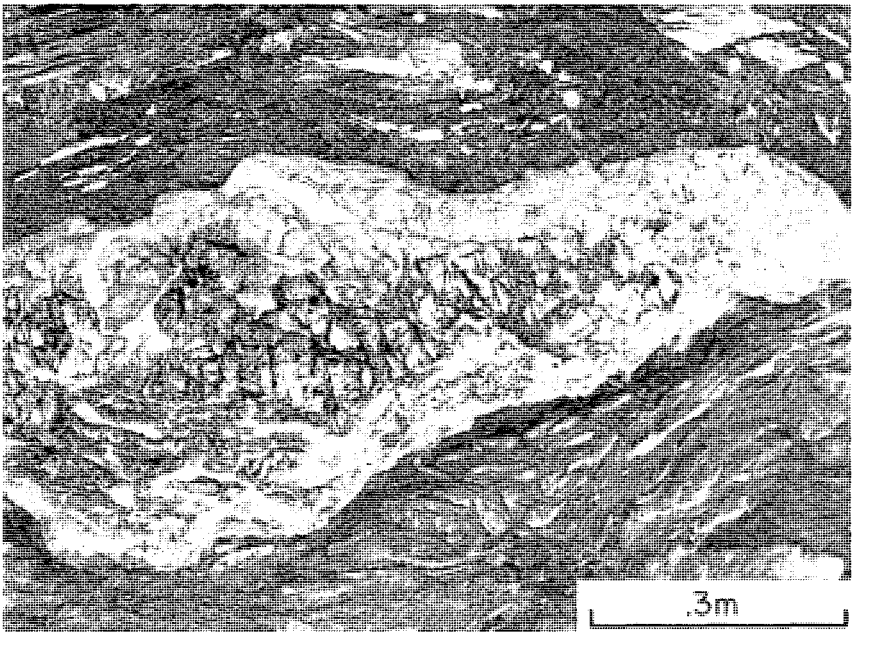

Figure 5. Boudinage in tectonic slice of marbleized limestone, unit I, plate I, looking north. Note the bedding-plane cleavage in shale which hosts the tectonic slice.

Limestone beds within unit 5 at the eastern end of the exposed part of the plate are folded about a series of overturned anticlines and synclines. These folds plunge gently north-northeast with axial surfaces striking northwest and dipping moderately northeast. To the northwest, these folds are truncated by the low-angle fault that forms the base of plate 4 (Plate 4). In the western part of plate 3, units 3 and 4, as well as the fault at the base of plate 3, are deformed by an overturned anticline and an overturned syncline. The axial surfaces of the folds dip approximately 35° NE. Both folds plunge approximately 30° N. Northwestward-directed flowage of limestone laminae is evident on the upper limb of the overturned anticline (Fig. 6). The low-angle fault at the base of plate 3 appears to cut gently down-section from the lower part of unit 4 on the east to unit 2 on the west. Plate 3 is truncated on the east by a north-northeast-striking, east-southeast-dipping, high-angle fault which forms a part of the western contact of plate 2 (Plate 4). The high-angle fault is slightly folded, which accounts for the apparent eastward projection of unit 5 of plate 3 into rocks of plate 2 (Plate 4). The area in the vicinity of this projection marks the convergence of plates 1 through 4 and is structurally complex.

Plate 2, containing units 2 to 5, is markedly discordant with respect to the other plates. In contrast to the preferred northwest-striking, gently northeast-dipping bedding that characterizes the rocks in plates 1, 3, 4, and 5, the strata in plate 2 dip steeply and strike north-northeast. In the north half of the exposed part of plate 2, the rocks are overturned and essentially homoclinal. To the south, the rocks are deformed in an unbroken series of tight anticlines and synclines, spaced at intervals of 1 to 3 m (Fig. 7). These folds plunge more steeply than those in the other plates; the orientation of axes ranges approximately 50° to 90° NE. Axial surfaces strike west-northwest and dip moderately to steeply northward. The south end of plate 2 is truncated by a west-northwest-striking, moderately north-northeast-dipping fault. Rocks of plate 1 form the footwall of this fault; their attitude is markedly discordant to bedding in plate 2 (Plate 4). To the east, plate 2 is separated from plate 1 by a bedding fault at the base of unit 2. Near the south end of plate 2, the fault cuts up-section to unit 3. At the north end of the exposed part of plate 2, rocks in plate 2 are truncated by the low-angle fault at the base of plate 5.

Plate 1 is best exposed in the southwest corner of the map area and consists predominantly of unit 1 with incorporated tectonic slices of units 2 and 3. Of all the plates, plate 1 is the most penetratively deformed. The shale is pervaded by bedding-plane cleavage and contains abundant overturned and isoclinal rootless folds of limestone, dolomite, and siltstone. Tectonic slices of limestone and dolomite have been sheared to a great extent. Faults unrecognizable in the highly deformed shale truncate and offset slices of brittle limestone. Plate 1 is a mixture of plates and tectonic slices.

In the southeast portion of the study area, the rocks and structures that comprise plate 1 are very poorly exposed. However, a sufficient number of bedding attitudes were obtained to disclose a large anticline, overturned to the northwest. This structure can be delineated by contrasting the steeply dipping, north-northeast-striking bedding attitudes near plate 2 with the northwest-striking, moderately northeast-dipping bedding attitudes that characterize plate 1 to the east (Plate 4). The π-axis of this fold plunges approximately 24° N 10° E; the attitude of the axial surface is approximately N 10° W, 56° E.

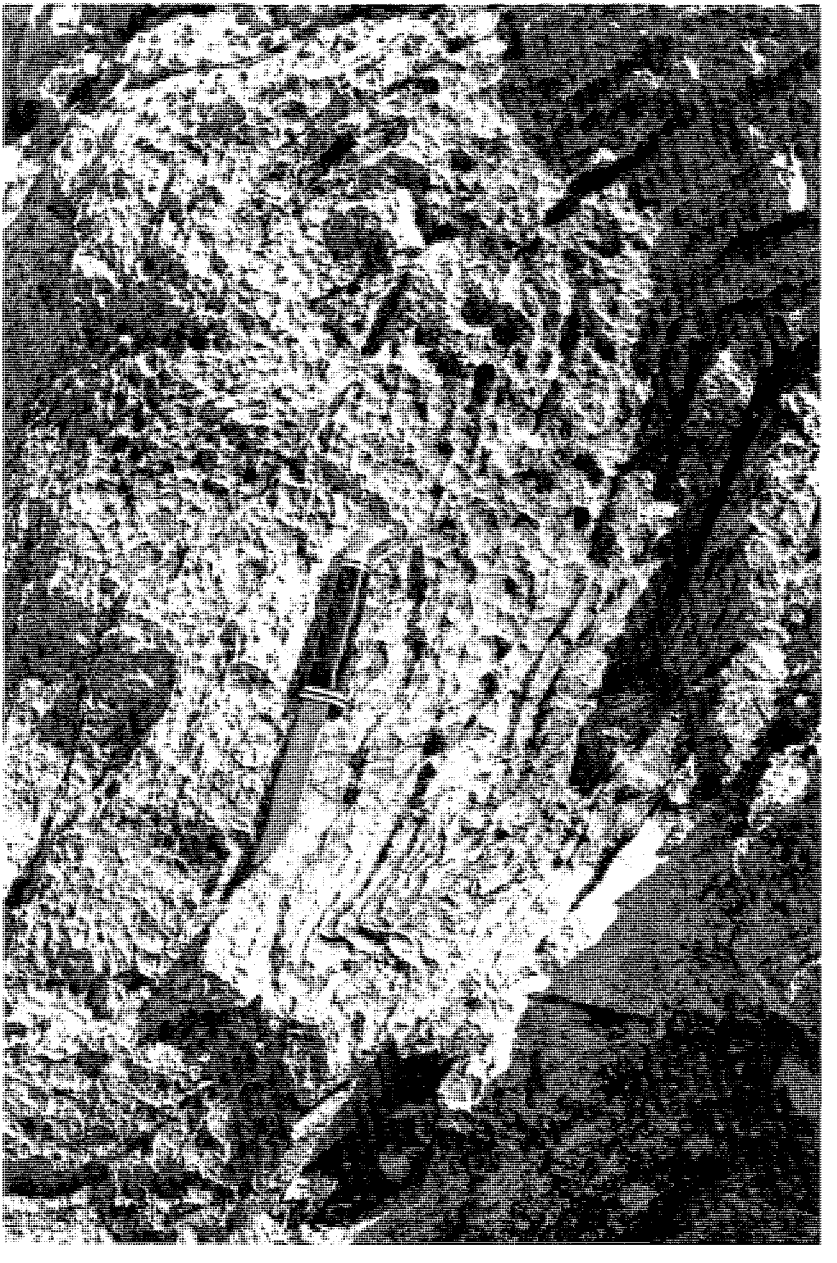

Figure 6. Overturned "cascade" fold defined by limestone laminae in unit 3, plate 3, looking northeast. Asymmetry of fold suggests northwest-directed movement.

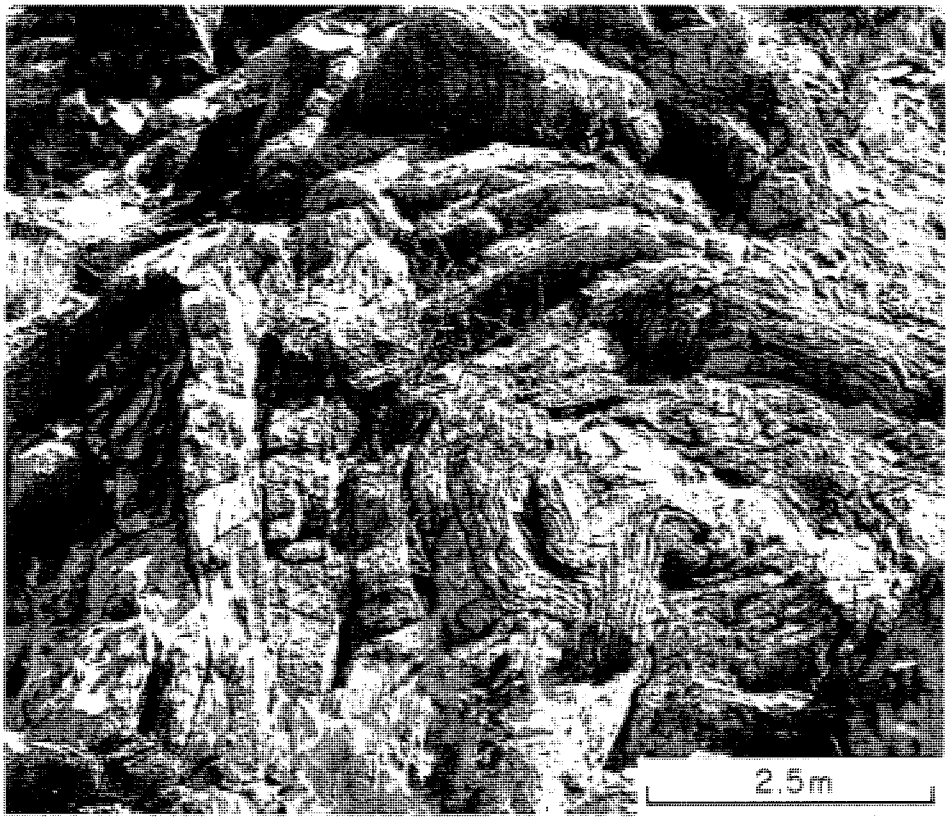

Figure 7. Complex fold pattern in southernmost exposed portion of plate 2, looking northeast.

Interpretation

The structural relationships exposed in the area appear to be a small-scale physical analog for Kehle's (1970) model of orogenic translation and gravity gliding. In his model of gravity gliding, Kehle assumes rock creep by simple shear to be the mechanism for inducing low-angle tectonic transport. Zones of low-viscosity rock become deforming strata (décollement zones) that effect rock transport through distributed shear. Transport of overlying, relatively high viscosity layers is accomplished by a conveyor-belt motion: the rocks are transported because of continuous deformation of underlying layers. Where resistance to flow occurs, folds and step thrust faults may form.

The structural assemblages that develop above and within a décollement zone are distinctly different from one another:

> Structures in the strata above a décollement zone develop independently of those within the zone. In the upper plate . . . step thrusts and folds form to overcome frontal buttressing. Structures within décollement zones include intensely developed passive disharmonic folds, bedding plane faults at contacts between high and low viscosity strata . . . , chaotic zones comprised of blocks of high viscosity strata, infolds of adjacent high viscosity strata, and penetrative cleavage, phylonitization, and other features of deformation-induced recrystallization (Kehle, 1970, p. 1641).

Although we cannot prove rigorously that Kehle's model was operative during the development of the structures mapped in the study area, the model is remarkably compatible with the deformation observed. In applying Kehle's model, the shale of unit 1 would comprise a décollement zone within which continuous deformation induced low-angle gliding of the overlying limestone. Evidence for ductile shearing of the shale is conspicuous in the pervasive cleavage. During discontinuous simple shear, thin beds of dolomite and siltstone within the shale section folded passively. With continued folding and attendant shearing, these relatively brittle layers were attenuated and dismembered, forming tectonic slices, chaotic blocks, and boudinage (Kehle, 1970, p. 1656).

Emplacement of plates 2-5, composed dominantly of limestone, may have been achieved through the repeated sequence of buttressing, folding, and step thrusting explicit in Kehle's model:

> Rocks comprising the upper plate of a thrust are originally continuous across the boundary that later becomes the forward edge of the thrust. This continuity of the rocks creates a buttress that prohibits motion of the thrust plate. If the plate begins to move, either a step fault forms at its forward edge, or the plate crumples against the buttress (Kehle, 1970, p. 1547).

A hypothetical sequence of progressive deformation for the rocks in the study area is illustrated in Figure 8. The sequence is intended to provide a general sense of the kinematics that may have attended the gravity gliding. Stage 5 of Figure 8 is a normal section that represents the present configuration of the five plates. In constructing this section, structural data were projected to a 60° SW-dipping plane oriented normal to the model orientations of bedding and fold axes. Given the postulated N 50° W-directed slip-line direction for the gravity-glide sheet in the Saguaro National Monument area (Davis, 1975) and the presumed original subhorizontal orientations of fold axes during gliding, the nor-

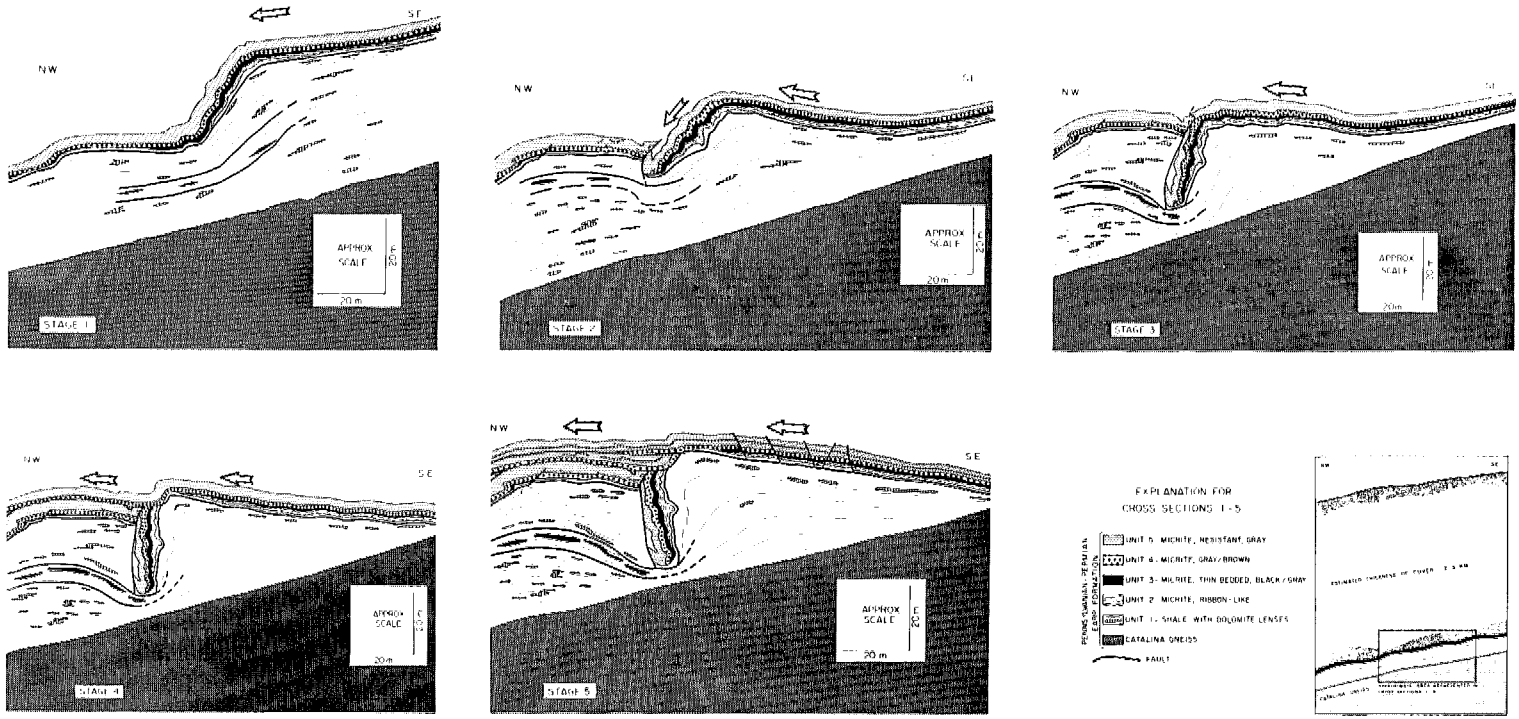

Figure 8. Inferred kinematic model for folding and emplacement of gravity-glide plates, Saguaro National Monument. Refer to text for explanation.

mal section shown in Figure 8 was chosen as the most appropriate basis for developing a kinematic model of the deformation.

The gravity gliding is inferred to have taken place beneath a cover of 2-3 km(?) in a regime whose gradient was controlled by the orientation of the northwest limb of Tanque Verde antiform (Fig. 8, stage 1). The load produced by a 2-3 km(?) overburden in conjunction with the 15-degree average slope angle of the Catalina fault may have triggered shear flow of unit 1 and transport of the overlying rocks, including units 2-5. Resistance to movement, brought about perhaps by a piling up of sedimentary layers to the northwest and/or a marked decrease in slope angle of the Catalina fault, is inferred to have resulted in flexing of the sedimentary rocks. Again extrapolating from Kehle's (1970, p. 1645) model, the "soft décollement zone rocks" in plate 1 may have moved into the growing anticline. Although originally only slightly asymmetrical, the fold is interpreted to have evolved into an overturned anticline as the result of (1) continued transport of (at least) units 2-5 and (2) continued flow of unit 1 shale into the anticlinal hinge zone. The net result of these coupled processes is inferred to have been a counterclockwise rotation of the anticlinal portion of the folded sheet and an underthrusting of the relatively high viscosity units (2-5) into the soft shale of plate 1 (Fig. 8, stages 2 and 3). The J-shaped drag fold at the foot of plate 2 in part records the movement of the middle limb of the originally unbroken asymmetric fold past the lower limb. Folds that had evolved in plate 2 prior to underthrusting acquired anomalously steep plunges and slightly divergent trends during the overturning and subsequent emplacement into plate 1.

Continued transport of units 2-5 toward the locus of overturning and rupture is inferred to have taken place as a result of sustained shear-flow within plate 1. Buttressing, in this case created by the presence of the rigid, vertically oriented plate 2, caused asymmetric folding in units 2-5. This folding was superseded by step thrusting which, in turn, induced the sequential emplacement of plates 4 and 5 (Fig. 8, stages 4 and 5). The pervasive bedding-plane cleavage noted in mudstone units within plates 4 and 5 suggests that a multiple décollement system was operative (at least) during the emplacement of plates 4 and 5 (Kehle, 1970, p. 1658). Shear flow in the mudstone layers provided increments of tectonic transport of parts of units 2-5 beyond that provided by the transport of the entire section of plate 1.

Conclusions

Large-scale geologic mapping and structural analysis of Paleozoic sedimentary rocks in a portion of Saguaro National Monument disclosed the presence of five small gravity-glide plates. Each plate is in fault contact with adjacent plates, and the boundary faults are locally folded. Limestone units within the deformed sequence display upright to overturned flexural-slip and flexural-flow folds. Shale-rich zones are pervaded by bedding-plane cleavage, tectonic slices, rootless folds, boudinage, and other forms of flow phenomena. In general, the pervasiveness and tightness of folds in limestone in each plate increase downward in the imbricate stack.

The apparent extreme structural complexity observed in rocks in the study area are explicable through application of Kehle's (1970) model of gravity gliding. Specifically, continuous shear flow of a shale-rich zone (décollement zone) induced transport of the overlying, more brittle rock units. The emergence of distinctive plates and a quadrupling of the section was brought about by buttressing and repeated step thrusting.

Acknowledgments

This study was carried out with the permission and cooperation of Saguaro National Monument headquarters. Harold T. Coss, Chief Park Naturalist, was particularly helpful to us and extended a sustained interest and encouragement. John P. Schloderer contributed in a meaningful way to the plane-table mapping of the study area, and we thank him for that. The Department of Geosciences, University of Arizona, defrayed field, travel, and drafting expenses.

References

Davis, G. H., 1973, Mid-Tertiary gravity-glide folding near Tucson, Arizona (abs.): Geol. Soc. America, Abstracts with Programs, v. 5, no. 7, p. 592.

_____1975, Gravity-induced folding off a gneiss dome complex, Rincon Mountains, Arizona: Geol. Soc. America Bull., v. 86, p. 979-990.

Davis, G. H., Frost, E. G., and Schloderer, J. P., 1974, Scrutiny of folded gravity-glide sheets in Saguaro National Monument, Arizona (abs.): Geol. Soc. America, Abstracts with Programs, v. 6, no. 5, p. 439.

Davis, G. H., Anderson, P., Budden, R. T., Keith, S. B., and Kiven, C. W., 1975, Origin of lineation in the Catalina–Rincon–Tortolita gneiss complex, Arizona: Geol. Soc. America, Abstracts with Programs, v. 7, no. 5, p. 602.

Drewes, Harald, 1975, Geologic map and sections of the Happy Valley quadrangle, Cochise County, Arizona: U.S. Geol. Survey Map I-832.

_____1973, Large-scale thrust faulting in southeastern Arizona (abs.): Geol. Soc. America, Abstracts with Programs, v. 5, p. 35.

_____1975, Preliminary geologic map of the Rincon Valley quadrangle, Pima County, Arizona: U.S. Geol. Survey Open-File Map, in press.

Kehle, R. O., 1970, Analysis of gravity gliding and orogenic translation: Geol. Soc. America Bull., v. 81, p. 1641-1664.

Mayo, E. B., 1964, Folds in gneiss beyond North Campbell Avenue, Tucson, Arizona: Arizona Geol. Soc. Digest, v. 7, p. 123-145.

McColly, R. A., 1961, Geology of the Saguaro National Monument, Pima County, Arizona: unpublished M.S. thesis, University of Arizona, Tucson, 80 p.

Moore, B. N., Tolman, C. F., Butler, B. S., and Kernon, R. M., 1941, Geology of the Tucson quadrangle, Arizona: U.S. Geol. Survey Open-File Report, 20 p.

Pashley, E. F., 1966, Structure and stratigraphy of the central, northern, and eastern parts of the Tucson Basin, Pima County, Arizona: unpublished Ph.D. dissertation, University of Arizona, Tucson, 273 p.